ENTROPY GENERATION ANALYSIS OF MHD MICROPOLAR NANOFLUID FLOW OVER A MOVED AND PERMEABLE VERTICAL PLATE

Abderaouf Mesbah

Mechanical Engineering, Biomaterials and Transport Phenomena Laboratory, ALGERIA

Reda Allouaoui

Mechanical Engineering, Biomaterials and Transport Phenomena Laboratory, ALGERIA

Amina Manal Bouaziz

Mechanical Engineering, Biomaterials and Transport Phenomena Laboratory, ALGERIA

Mohamed Najib Bouaziz[*]

Mechanical Engineering, Biomaterials and Transport Phenomena Laboratory, ALGERIA
E-mail: mn_bouaziz@email.com

The goal of this paper is to learn more about how a magnetic field, Brownian motion, and thermophoresis diffusion influence convective heat transfer in a micropolar-nanofluid flow's laminar boundary layer. Near a vertically moving, permeable plate, the complex fluid is subjected to MHD. The MATLAB application bvp4c was utilized to simplify the governing nonlinear and coupled equations for the micropolar-nanofluid, leading to the solution of the ensuing ordinary differential equations (ODEs). Graphs have been used to analyze the effect of different relevant active factors on the flow field and temperature. The results demonstrate that the micro-rotation of the nanoparticles taken into account and in suspension becomes significant for the complex fluid in the presence of the magnetic field. Analysis of the generation entropy shows that the surface is a significant source of irreversibility. There is no discernible effect of micropolarity on the relationship between Brownian and thermophoresis numbers and entropy generation.

Key words: entropy analysis, magnetohydrodynamic, micropolar-nanofluid, micro-rotation, moved plate.

1. Introduction

Because of their higher thermal conductivity, nanofluids have been developed in recent decades to replace traditional fluids. These nanofluids are made up of a base fluid and nanoparticles of metals and oxides. As a result, a wide range of applications can be put to good use, and the ongoing difficulties of enhancing heat transfer can be surmounted.

Adding nanoparticles to a fluid increases its ability to conduct heat transfer [1], but also raises its viscosity and, by extension, its pressure drop. The best circumstances of energy consumption can be determined by calculating the entropy of a system and minimizing it, which paves the way for maximum efficiency through reduced energy waste.

Some current studies on the entropy created by fluids can be summed up here. Entropy formation in the trapezoidal cavity was reduced by Mondal and Mahapatra [2] by balancing the influences of fluid movement, heat transfer, mass transfer, and the magnetic field. Abbasi *et al.* [3] analyzed the entropy generation during peristalsis of a nanofluid whose viscosity varies with temperature. In order to generate

---

[*] To whom correspondence should be addressed

entropy for an MHD water-based Fe_3O_4 ferrofluid, Shafee *et al.* [4] used a computational fluid dynamics (CFD) finite element model (CFEM) in a porous semi-annulus cavity. The second law analysis of a Powell-Eyring fluid moving via an angled microchannel was studied by Madhu *et al.* [5]. Madhu *et al.* [6] analyzed the heat transfer and entropy generation of a non-Newtonian fluid flowing in a vertical microchannel with a convective boundary condition. The entropy-generating peristaltic flow of AgH_2O nanofluid was the subject of research by Akbar *et al.* [7]. The effects of viscous dissipation and a varying magnetic field were taken into consideration in a computer study on entropy analysis in amixed convection MHD flow of ananofluid over a non-linear stretched sheet by Martin *et al.* [8]. Nanofluid turbulent forced convection was studied by Bianco *et al.* [9] using a parametric analysis to determine the entropy generation in a tube with a circular cross-section and a constant wall heat flux. Poiseuille nanofluid flow with slip and convective boundary conditions in a porous channel subjected to a magnetic field was studied by Das *et al.* [10]. A radiative MHD Casson nanofluid flow with activation energy and chemical reaction across a previously nonlinearly stretched surface was presented by Shah *et al.* [11]. Entropy generation study of eccentric cylinders pair sources on nanofluid natural convection in a non-Boussinesq state was investigated by Mirzaee and Laksaian [12]. Under the influence of MHD and heat radiation, Hosseinzadeh *et al.* [13] conducted an entropy generation investigation of a nanofluid comprising CNTs and $(CH_2OH)_2$. Ibáez *et al.* [14] investigated the movement of a viscous electrically conducting nanofluid via a microchannel containing permeable plates. The final conclusion was the result of the integration of several effects, including convective boundary conditions, thermal radiation, suction/injection, magnetic field, hydrodynamic slip, and nanoparticle volume fraction. Entropy analysis in an electrical magnetohydrodynamic (MHD) flow of a nanofluid under the influence of thermal radiation was studied by Daniel *et al.* [15]. Hussain *et al.* [16] investigated the entropy creation of a water-alumina nanofluid flow in a double lid driven cavity with discontinuous heating. Entropy generation study during MHD natural convection flow of a hybrid nanofluid in a square cavity with a corrugated conducting block was studied numerically by Tayebi and Chamkha [17].

Many engineering tasks benefit from the use of non-Newtonian fluids with convective heat transfer. A strain-stress relationship that is not linear is used to model these fluids with non-linear constitutive behavior. Some of these fluids, known as micropolar fluids, play an essential part in the technical developments across a wide range of industries, thanks to their beneficial performance in areas like naval and aeronautical engineering, telecommunications, energy production systems, and the food sector. In other way, taking into account the rotations of particles, nanoparticles or molecules constituting a complex fluid is particularly supported by the micropolar fluid, seen as a representative mathematical model.

Magnetohydrodynamics (MHD) has received a lot of attention as of late, too. MHD is concerned with the movements of electrically conductive fluids in the presence of electric and magnetic fields. When a fluid that conducts electricity moves through a magnetic field, the fluid's motion is affected by induced electric currents that, in turn, cause mechanical forces as they interact with the initial magnetic field. The effects of viscous dissipation, mixed convection, velocity slip, and temperature jump on the flow of a micropolar nanofluid were studied by Roja *et al.* [18]. Considering magnetic effects and heat production/absorption, Javed and Siddiqui [19] analyzed the linear stability of micropolar nanofluid flow via entrapped triangular enclosures using a mixed convection model. Javed *et al.* [20] investigated the effect of MHD on mixed convection in a triangular permeable cavity filled with micropolar nanofluid-saturated porous media. Chand *et al.* [21] analyzed the rule of linear stability hypothesis in their theoretical examination of thermal convection in a horizontal layer of micropolar nanofluid. Yusuf *et al.* [22] give an investigation of the irreversibility of a micropolar fluid film moving down an inclined porous substrate with slip effect. Squeezing flow of a Casson-micropolar nanofluid with injection/suction and slip effects was studied by Ramesh *et al.* [23]. Nonlinear thermal radiation and activation energy were applied to a porous rotating disk containing swarming microorganisms in a study by Ijazkhan *et al.* [24]. However, research into the use of nanofluids in conjunction with a micropolar fluid as the basis fluid is yet limited. In this context, referencing relevant findings is appropriate. In their research, Eid and Mabood [25] considered heat sources/sinks and thermal radiation while studying the magnetohydrodynamics of a micropolar dusty nanofluid impinging on an expanding sheet in a porous regime. The most notable results include a decrease in flow velocity and temperature with an increase in the suction parameter, and the opposite

for the injection. According to the research of Roja *et al.* [18], entropy production is increased by the angle of inclination and the Grashof number and decreased by the material parameter and the magnetic parameter. Entropy formation on the boundary layer over a stretching surface and a chemical reaction were studied by Almakki *et al.* [26] in the context of a micropolar nanofluid of MHD fluid. They discovered that thermal diffusion is the most important contributor to entropy formation, and that the process becomes more efficient at higher Reynolds and Brinkman numbers. Micropolar magnetite-Fe_3O_4 Ferro-liquid was studied in depth by Zaib, *et al.* [27], employing mixed convective flow from a vertical plate. They found that the micropolar parameter speed up the boundary-layer separation while the volume percentage of ferroparticles slowed it down. Nayak *et al.* [28] examine the incompressible unsteady flow of a micropolar cross nanofluid in a magnetic field past a linear stretching/shrinking sheet. Heat and mass fluxes are accounted for according to the Cattaneo-Christov diffusion theory. Increase in the stretching/shrinking strength parameter increases the irreversibility ratio.

It is possible to represent the boundary layer flow and the heat transfer across a constantly moving surface as a stretched sheet responsive to heat transfer. Extruding plastic sheets or other forms of working with polymers exhibits the stretched sheet phenomena. Therefore, the surface velocity is critical since it directly affects the rate of heat transmission. The heat transfer rate from the permeable plate can be affected by the flow field if a fluid is sucked or injected through the bounding surface, as in mass transfer cooling. The author is unaware of any previous research involving the use of numerical simulation to examine the creation of entropy on a micropolar nanofluid under MHD and passing through a movable and permeable plate. Such useful experiments can be performed under these circumstances.

This work analyzes the creation of entropy during the free convection MHD flow of a micropolar nanofluid down a vertical, permeable, and movable plate, factoring in the dissipation due to viscosity. The convenient micropolarity is a mathematical approach that adequately represents the rotating of the nanoparticles of the fluid. A complex problem simulation calls for a tailored mathematical framework and precise numerical approach. The resulting system of boundary layer equations based on the heterogeneous Buongiorno model is transformed into an ordinary differential equation system via similarity transformation. Then, using the bvp4c function in Matlab, they are numerically solved. The effects of the magnetic field, Brownian motion, and thermophoresis on the located entropy created will be illustrated graphically using selected results.

2. Mathematical analysis

It is assumed that an incompressible micropolar nanofluid is flowing laminarly convectively along a vertical plate with a semi-infinite thickness. The plate is subjected to a normal B_x transverse magnetic field.
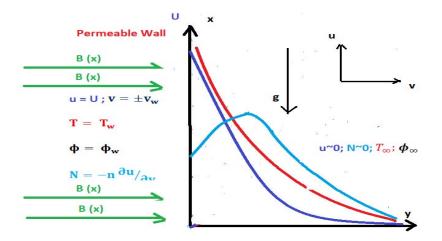

Fig.1. The simplified representation of the current physical problem.

Dissipation of magnetic energy is taken into account. The fluid enters and exits the plate at a transverse velocity v_w, while the plate itself moves at a constant x-direction velocity U. The ambient temperature and nanoparticle volume fraction increase as y approaches infinity, but the wall at the vertical plate (T_w and φ_w) maintains a constant value, assuming that these are greater than the ambient temperature and the ambient nanoparticle volume fraction attained as y tends to infinity (T_∞ and φ_∞, respectively). The flow is in the same direction as the x-axis, and the y-axis is perpendicular to the plate. In Fig.1 we see a simplified representation of the current physical problem.

It is helpful to provide two methods for calculating the entropy generation before offering the mathematical formulation. If the friction factor and the Nusselt number have classical relationships, then the total entropy generation of the system can be calculated. This method can only be used for internal flows.

In the other and more precise method, local entropy generation can be determined for each component of the system under study. For the micropolar nanofluid, you need to write and solve equations for the momentum, angular momentum, energy, and volume fraction of the nanoparticles. The local and total entropy generations are then calculated for each location in the domain using the velocity, angular velocity, and temperature fields. Then we may assess the practical quantities that matter.

The mass, momentum, angular momentum, energy, and volume fraction of nanoparticles conservation equations for the given situation can be expressed as

$$\frac{\partial u}{\partial x} + \frac{\partial u}{\partial y} = 0, \tag{2.1}$$

$$u\frac{\partial u}{\partial x} + v\frac{\partial u}{\partial y} = \left(\frac{\mu + \kappa}{\rho}\right)\frac{\partial^2 u}{\partial y^2} + \frac{\kappa}{\rho}\frac{\partial N}{\partial y} + g\beta(T - T_\infty) - \frac{\sigma B_0^2}{\rho}u, \tag{2.2}$$

$$j\rho\left(u\frac{\partial N}{\partial x} + v\frac{\partial N}{\partial y}\right) = \gamma\frac{\partial^2 N}{\partial y^2} - \kappa\left(2N + \frac{\partial u}{\partial y}\right), \tag{2.3}$$

$$u\frac{\partial T}{\partial x} + v\frac{\partial T}{\partial y} = \propto_{nf}\frac{\partial^2 T}{\partial y^2} + \frac{(\rho c)_p}{(\rho c)_f}\left(D_B\frac{\partial \varphi}{\partial y}\frac{\partial T}{\partial y} + \frac{D_T}{T_\infty}\left(\frac{\partial T}{\partial y}\right)^2\right) + \frac{\sigma B_0^2}{(\rho c)_f}u^2, \tag{2.4}$$

$$u\frac{\partial \varphi}{\partial x} + v\frac{\partial \varphi}{\partial y} = D_B\frac{\partial^2 \varphi}{\partial y^2} + \frac{D_T}{T_\infty}\left(\frac{\partial T}{\partial y}\right)^2. \tag{2.5}$$

We observe that N is the component of the microrotation vector normal to the x-y plane, and T is the temperature in the boundary layer. According to the work of Hsiao, [29], the spin gradient viscosity is $\gamma = (\mu + \kappa / 2)j$.

The boundary conditions are:

$$\text{at } y = 0: \ u = U; \ v = \pm v_w; \ T = T_w; \ \varphi = \varphi_w \quad \text{and} \quad N = -n\,\partial u / \partial y, \tag{2.6}$$

$$\text{for } y \to \infty: \ u \to 0; \ T \to T_w; \ \varphi \to \varphi_w \quad \text{and} \quad N \to 0 \tag{2.7}$$

where n is assumed equal to ½ for weak concentration [30].

Introducing the dimensionless quantities and the similarity variables, as in Yacob and Ishak [30]:

$$\eta = (U / \nu x)^{1/2} y; \quad \psi = (\nu x U /)^{1/2} f(\eta); \quad N = (U / \nu x)^{1/2} h(\eta), \tag{2.8}$$

$$\theta = (T - T_\infty) / (T_w - T_\infty), \quad S = (\phi - \phi_\infty) / (\phi_w - \phi_\infty), \tag{2.9}$$

$f(\eta)$ is the dimensionless stream function, $h(\eta)$ is the dimensionless microrotation, $T(\eta)$ is the dimensionless temperature and $S(\eta)$ is the nanoparticle volume fraction. the independent similarity variable is represented by η. The stream function denoted by ψ, is defined as follows: $u = \partial\psi / \partial y$ and $v = -\partial\psi / \partial x$ j have taken $j = \nu x / U$ as the micro-inertia density.

The velocity components become

$$u = U f'(\eta) \quad \text{and} \quad v = \frac{1}{2}(\nu x / x)^{1/2}(\eta f' - f). \tag{2.10}$$

By applying the similarity transformation parameters, the system of equations can be reduced to

$$(1 + K) f''' + \frac{1}{2} f \cdot f'' - M \cdot f' + K \cdot h' + Gr_x \cdot \theta = 0, \tag{2.11}$$

$$\left(1 + \frac{K}{2}\right) h'' - K(2h + f'') + \frac{1}{2}(h \cdot f)' = 0, \tag{2.12}$$

$$\theta'' + \frac{1}{2} Pr \cdot f \cdot \theta' - Nb \cdot S' \cdot \theta' - Nt(\theta')^2 + M \cdot Ec \cdot Pr \cdot f'^2 = 0, \tag{2.13}$$

$$S'' + \frac{1}{2} Pr \cdot Ln \cdot f \cdot S' + \frac{Nt}{Nb} \theta'' = 0. \tag{2.14}$$

The boundary conditions become

$$\eta = 0: \ f'(0) = 1; \ f(0) = \pm f_w; \ h(0) = -\frac{1}{2} f''(0); \ \theta(0) = S(0) = 1, \tag{2.15}$$

$$\eta \to \infty: \ f'(\infty) = 0; \ h(\infty) \to 0; \ \theta(\infty) \to 0; \ S(\infty) \to 0. \tag{2.16}$$

The following numbers are defined as

$$Gr_x = g\beta(T_w - T_\infty) x / U^2, \tag{2.17}$$

$$K = \kappa / \mu, \tag{2.18}$$

$$Ln = \alpha_{nf} / D_B, \tag{2.19}$$

$$Nb = (\rho c)_p D_B (\phi_w - \phi_\infty) / (\rho c)_f \alpha_{nf}, \tag{2.20}$$

$$Nt = (\rho c)_p \, D_T \left(T_f - T_\infty \right) / (\rho c)_f \, T_\infty \alpha_{nf} \, , \tag{2.21}$$

$$M_x = Ha_x^2 / Re_x = \sigma B_0^2 x / \rho U \, , \tag{2.22}$$

$$E_C = U^2 / c_p \left(T_w - T_\infty \right) , \tag{2.23}$$

$$Pr = \nu / \alpha_{nf} \, . \tag{2.24}$$

3. Entropy generation analysis

In a closed system, irreversible internal mechanisms initiate a computation that results in the production of entropy. Ignoring the dissipations due to the Brownian motion and the thermophoresis, the local volumetric rate of entropy generation in a magnetic field for nanofluids can be given as [31].

$$EG = \frac{k_{nf}}{T_m^2}\left(\frac{\partial T}{\partial y}\right)^2 + \left(\frac{\mu + \kappa}{T_w}\right)\left(\frac{\partial u}{\partial y}\right)^2 + \left(\frac{2\kappa}{T_w}\right)\left(N^2 + N\frac{\partial u}{\partial y}\right) + \left(\frac{\gamma}{T_w}\right)\left(\frac{\partial N}{\partial y}\right)^2 + \frac{\sigma B_0^2}{T_w}u^2 \, . \tag{3.1}$$

Five sources considered in the Eq.(3.1) contribute to the generation of entropy, the first term refers to conduction effect which is known as heat transfer irreversibility (HTI), the other terms are the fluid friction irreversibility (FFI) due to natural viscous dissipation of the fluid, to complex material and gyration dissipation caused by the microrotation and micro-inertia of the fluid, and entropy generated by the magnetic field.

Ns, the number of entropy generation, is defined as the ratio of the local volumetric entropy generation rate to a characteristic entropy generation rate, and is introduced to better understand and study the addition of some other effects on the entropy generation.

The entropy generation number is defined

$$N_s = \frac{EG}{EG_0} \tag{3.2}$$

where $EG_0 = \dfrac{U^2}{T_w}\left(\sigma B_0^2\right)$ here, is the characteristic entropy generation rate adopted.

Then, using Equations (2.8), (2.9), (3.1) and (3.2) entropy generation number reduce to

$$N_s = \frac{4}{Br\Omega M_x}\frac{\theta'^2}{(\theta-1)^2} + \frac{(1+K)}{M_x}f''^2 + \frac{2K}{M_x}\left(h^2 + hf''\right) + \frac{1}{M_x}\left(1 + \frac{K}{2}\right)h'^2 + f'^2 \tag{3.3}$$

where *Br* denotes the Brinkman numbers, Ω is the dimensionless temperature difference. These numbers are:

$$Br = \frac{\mu u_w^2}{k_{nf}\Delta T}, \quad \Omega = \frac{\Delta T}{T_\infty} \quad \text{and} \quad M_x = \frac{\sigma B_0^2}{\rho U}x \, . \tag{3.4}$$

4. Numerical method

Since the non-Newtonian fluid is involved, especially in the energy equations, the numerical method planned for the simulation of the complex problem requires additional care.

Closed form solutions for the set of coupled ordinary differential equations (2.11) and (2.14) with their boundary conditions (2.15) and (2.16) are unattainable due to their highly non-linear and linked nature. They have a numerical solution. Using a finite difference technique, numerical Runge-Kutta methods are able to solve ordinary differential equations, making the resulting algebraic system tractable. The RK list is rounded up by a few more classes in addition to the specified primary forms. A class of methods known as embedded methods differs from the implicit class of Lobatto method families in that they aim to generate a local truncation error estimate for a single Runge Kutta step instead of a global estimate, which makes them less accurate. At the start and finish of every integration subinterval, estimates of the solution are calculated using the trapezoidal quadrature rule.

This can be done with the @Matlab code bvp4c. Here, the process yields a continuous solution with consistent fourth-order accuracy over the integration interval by using the Lobatto IIIa collocation formula and collocation polynomial applied by the finite difference method. By utilizing the continuous solution's residual, we can choose a suitable mesh and control errors. Until the outcome satisfies the tolerance requirements, the interval of integration is divided into smaller intervals using the mesh of points created by the collocation technique. The calculations were performed after some careful selections were made regarding the initial solution vector, the mesh by size with $\Delta\eta = 0.001$, and the infinity terminal point. A convergence criterion of 10^{-5} was selected to ensure that the results fully satisfy the boundary condition, that is, the far field asymptotic values are satisfied. Ultimately, the entropy generation number, or Eq. (3.3), is obtained by using the boundary layers.
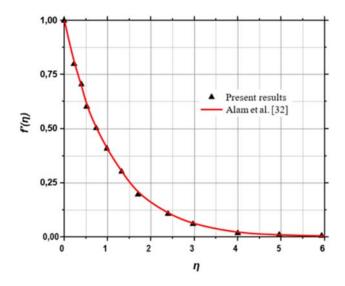

Fig.2. Comparisons with present velocity profile $f'(\eta)$ and results of Alam *et al.* [32].

Numerical results for dimensionless velocity have been compared to these of Alam *et al.* [32], for a permeable flat plate in the absence of a magnetic field, mass transfer given by these authors, and nanoparticles in the present code, to guarantee that the code implemented works and is free of mistakes. As can be seen in Fig.2, the two sets of data agree quite well.

5. Results and discussions

Thermophysical factors govern the flow zones. All figures represent the results of numerical simulations performed for a range of values of the parameters displayed.

Here, we present the findings in graphical formats. We are particularly interested in the micropolar parameter K, the Prandtl number Pr, the Eckert number Ec, the thermophoretic parameter Nt, and the Brownian motion parameter Nb, all of which are physical dimensionless values.

5.1. Effect of *M* and *K* on the profiles

Figure 3 displays $f'(\eta)$ velocity profiles for a range of the magnetic parameter *M* values. It is observed that the velocity of the nanofluid reduces as the magnetic field *M* increases for a range of values. When a nanofluid is subjected to a transverse magnetic field *M*, it experiences a Lorentz force, a sort of resistive force that tends to slow down the flow. The magnetic field *M* acts as a drag on the mixed convection flow, increasing the local coefficient of friction. It is interesting to note, from the perspective of the fluid's micropolarity, that the thickness of the hydrodynamic layer increases as the micropolarity of the fluid *K* increases. The physics of flows is thus confirmed by these findings.
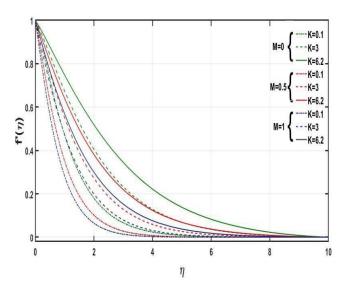

Fig.3. Velocity profiles $f'(\eta)$ for *Gr$_x$ = 2.0, Pr = 6.2, Nb = 0.1, Nt = 0.1, Ec = 0.1, Ln = 2.0* and different *M*.
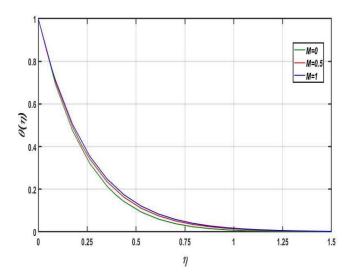

Fig.4. Temperature profiles $\theta(\eta)$ for *Gr$_x$ = 2.0, K = 0.1, Pr = 6.2, Nb = 0.1, Nt = 0.1, Ec = 0.1, Ln = 2.0* and different *M*.

In Fig.4, we see the dimensionless temperature profiles $\theta(\eta)$ for the change in the magnetic parameter *M*. Due to the heat dissipation generated by the magnetic field, the thermal boundary layer expands by a factor

of 4 as the magnetic parameter *M* is raised. The temperature profile clearly demonstrates a struggle between the displaced plate and natural convection.
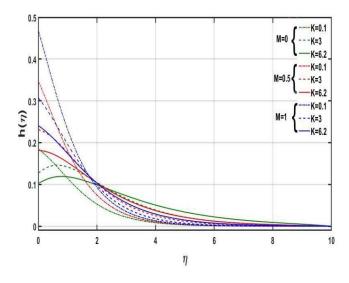

Fig.5. Microrotation profiles $h(\eta)$ for $Gr_x = 2.0$, $Pr = 6.2$, $Nb = 0.1$, $Nt = 0.1$, $Ec = 0.1$, $Ln = 2.0$ and different *M*.

In Fig.5, we can see that the micropolarity at each field strength moderates the magnetic field's incidence on the microrotation's levels. At $\eta = 1.0$ and $\eta = 2.0$, we see an inflection in both curves as *M* grows, so does the microrotation close to the plate, but beyond a certain distance from the wall, the number of the magnetic parameters has no effect on the angular velocity.

5.2. Effect *Pr* and *K* on the profiles

The velocity profiles $f'(\eta)$ for various values of the Prandtl number *Pr* are shown in Fig.6. Kinematic viscosity, momentum diffusivity, and thermal diffusivity are all compared using the Prandtl number *Pr*.
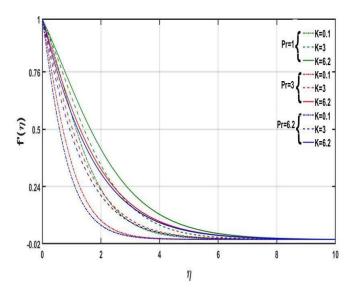

Fig.6. Velocity profiles $f'(\eta)$ for $M = 1$, $Gr_x = 2.0$, $Nb = 0.1$, $Nt = 0.1$, $Ec = 0.1$, $Ln = 2.0$ and different *Pr*.
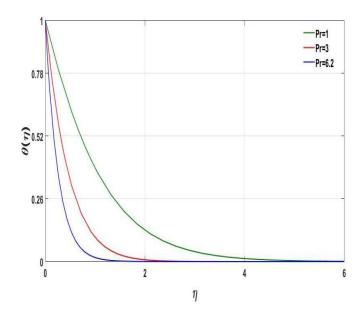
Fig.7. Temperature profiles $\theta(\eta)$ for *M = 1, Gr$_x$ = 2.0, K = 0.1, Nb = 0.1, Nt = 0.1, Ec = 0.1, Ln = 2.0*
and different *Pr*.

If the Prandtl number *Pr* is high, then the temperature profile of the fluid will be highly sensitive to the flow rate. In this example, the velocity drops dramatically as one moves towards the hydrodynamic boundary layer. When the fluid has a high micropolarity, making it denser than a Newtonian fluid, this trend breaks down.

Numerical results reveal that low *Pr* has a significant impact on the heat transfer process, as depicted in Fig.7, where the thickness of the thermal boundary layer drops and the temperature distribution spreads out quickly in the corresponding boundary layer.

The microrotation profile $h(\eta)$ is shown in Fig.8 for a range of *Pr* values; similar to the curves described in Fig.5, an increase in Prandtl number *Pr* suggests a decrease in the microrotation profile $h(\eta)$.
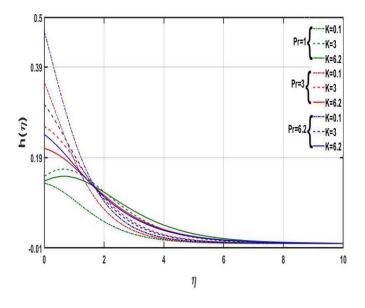

Fig.8. Microrotation profiles when *M = 1, Gr$_x$ = 2.0, Nb = 0.1, Nt = 0.1, Ec = 0.1, Ln = 2.0* and different *Pr*.

5.3. Entropy rate profiles

For a range of values of the magnetic parameter M, the profile of the entropy generation number Ns is depicted in Fig.9. The entropy generation Ns close to the wall rises in proportion to the value of the magnetic parameter M, while the entropy generation at further distances from the wall is relatively unaffected. But it is quite strong up against the wall. Heat is dissipated in a fluid volume interacting with many phenomena because an increase in the magnetic parameter creates resistance forces against the motion of the fluid. Consequently, the irreversibility of friction has a major bearing on the velocity of the fluid.

Eckert numbers Ec and Ns are discussed in relation to Fig.10 for a range of values. This is because fluid friction near the plates has a significant and irreversible effect. The importance of thermal irreversibility is highlighted by the figure; this is especially true in the region closest to the wall, where the temperature differential is quite small. Ec has half as much of an impact as M does.

The curves of Ns are shown in Fig.11 for varying values of the material parameter K. The graph shows that there is little to no difference between the two groups, especially when looking at the projected curves, suggesting that micropolarity has little effect on the entropy generation. At a distance > 0.35, Ns decreases to almost nothing. It is well-established that entropy is always positive and that it is created in close proximity to the boundary.

Figures 12 and 13 show the impact of the thermophoretic parameter and the Brownian parameter on the entropy generation number. Increases in these two parameters cause an equivalent rise in the temperature profile, whereas an increase in temperature causes an equivalent rise in the two diffusion parameters, resulting in lower Ns close to the plate (the source of the nanoparticles' displacement). Because these mechanisms do not go very far away from the plate, they generate very little entropy.
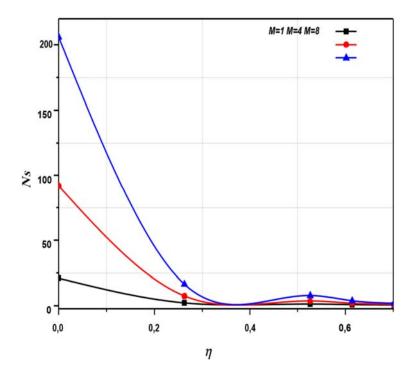

Fig.9. Profiles of entropy generation number Ns for $Ec = 0.1$, $Pr = 6.2$, $M = 1$, $Gr = 2.0$, $Nb = 0.1$, $Nt = 0.1$, $K = 0.1$, $Ln = 2$, $Br \cdot \Omega = 1$ and different M.
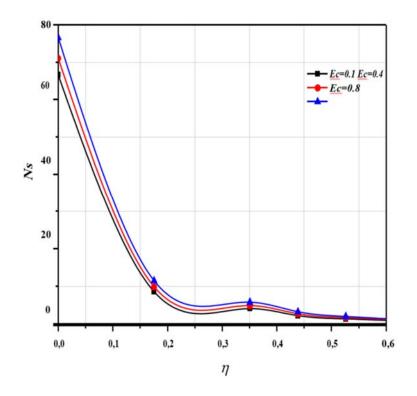
Fig.10. Profiles of entropy generation number *Ns* for $M = 1$, $Pr = 6.2$, $Gr = 2.0$, $Nb = 0.1$, $Nt = 0.1$, $K = 6$, $Ln = 2$, $Br \cdot \Omega = 1$ and different *Ec*.
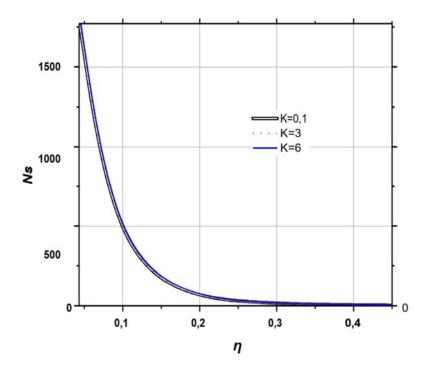

Fig.11. Profiles of entropy generation number *Ns* for $M = 1$, $Ec = 0.1$, $Pr = 6.2$, $Gr = 2.0$, $Nb = 0.1$, $Nt = 0.1$, $Ln = 2$, $Br \cdot \Omega = 1$ and different *K*.

Fig.12. Profiles of entropy generation number *Ns* for *M = 1*, *Ec = 0.1*, *Pr = 6.2*, *Gr = 2.0*, *Nb = 0.1*, *Ln = 2*, $Br \cdot \Omega = 1$ and different *Nt*.

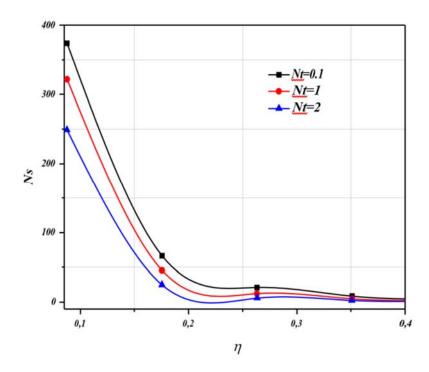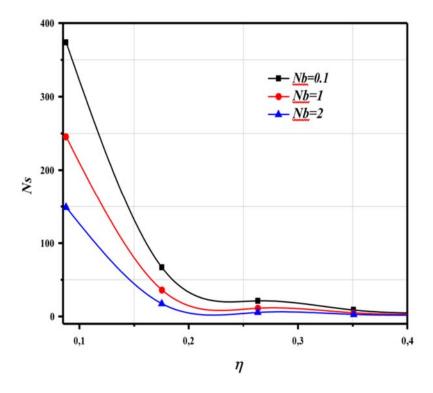Fig.13. Profiles of entropy generation number *Ns* for *M = 1*, *Ec = 0.1*, *Pr = 6.2*, *Gr = 2.0*, *Nt = 0.1*, *Ln = 2*, $Br \cdot \Omega = 1$ and different *Nb*.

6. Conclusions

A numerical solution of entropy production is studied in for a nano-micropolar fluid next to a movable and permeable plate subject to a magnetic field. Using a permeable vertical plate as an example, governing equations are derived for constant laminar micropolar nanofluid flow, convective heat and nanoparticle transfer. The controlling partial differential equations are transformed using a similarity transformation into ordinary ones, and then solved numerically using Lobatto III discretisation and bvp4c. The parameters material, Eckert number, and Prandtl number, as well as the effects of the magnetic field, are all thoroughly explored. The rates at which entropy can be generated are also underlined. The data demonstrate:

- In spite of the fact that a magnetic field may be used to slow things down in the boundary layer, additional microrotation of the nanofluid is anticipated, albeit attenuated by the micropolarity.
- Near the plate, where substantial irreversibility occurs, entropy generation is basically more intense.
- A high Eckert number or an external magnetic field both have the effect of boosting entropy formation.
- Changing the fluid's micropolarity has no appreciable effect on *Ns*.
- The wall's entropy generation decreases as Brownian and thermophoresis velocities increase.
- Insights into the heat and fluid dynamics of the suggested micropolar-nanofluid linked with a moving and permeable plate and subject to the MHD effect have been gained by the present computations. Furthermore, the entropy can be minimized to enable the designer plan for best conditions, leading to tangible outcomes.

Acknowledgements

Nomenclature

$B(x)$ – magnetic field

B_0 – constant magnetic field

Br – Brinkman number

c – specific heat at constant pressure

D_B – Brownian diffusion coefficient

D_T – thermophoretic diffusion coefficient

Ec – Eckert number

EG – local volumetric rate of entropy generation

f – dimensionless stream

g – gravity

Gr – Grashof number

h – dimensionless microrotation

Ha – Hartman number

j – micro-inertia density

k – thermal conductivity

K – material parameter

M – magnetic parameter

n – constant

N – microrotation velocity

Nb	– Brownian diffusion parameter
Nt	– thermophoretic diffusion parameter
Ns	– entropy generation number
Pr	– Prandtl number
Re	– Reynolds number
S	– dimensionless nanoparticle volume fraction
T	– temperature
ΔT	– difference temperature
u	– velocity in x-direction
U	– constant velocity of the plate
v	– velocity in y-direction
α	– thermal diffusivity
β	– volumetric thermal expansion coefficient
γ	– spin gradient velocity
η	– similarity variable
κ	– vortex viscosity
μ	– dynamic viscosity
ν	– kinematic viscosity
ρ	– density
ρc	– heat capacitance
σ	– electrical conductivity of the fluid
φ	– nanoparticle volume fraction
Ψ	– stream function
Ω	– dimensionless temperature difference
θ	– dimensionless temperature

References

[1] Moghaddami M., Seyedehsan E.S., and Siavashi M. (2012): *Entropy generation analysis of nanofluid flow in turbulent and laminar regimes.–* Journal of Computational and Theoretical Nanoscience, vol.9, pp.1586-1595. https://doi.org/10.1166/jctn.2012.2249

[2] Mondal P. and Mahapatra T.R. (2021): *MHD double-diffusive mixed convection and entropy generation of nanofluid in a trapezoidal cavity.–* International Journal of Mechanical Science, vol.208, pp.106-655. https://doi.org/10.1016/j.ijmecsci.2021.106665

[3] Abbasi F.M., Shanakhat I. and Shehzad S.A. (2019): *Entropy generation analysis for peristalsis of nanofluid with temperature dependent viscosity and Hall effects.–* Journal of Magnetism and Magnetic Materials, vol.474, pp.434-441, https://doi.org/10.1016/j.jmmm.2018.10.132

[4] Shafee A., Haq R.U., Sheikholeslami M., Herki J.A.A. and Nguyen T.K. (2019): *An entropy generation analysis for MHD water based Fe_3O_4 ferrofluid through a porous semi annulus cavity via CVFEM.–* International Communications in Heat and Mass Transfer, vol.108, pp.104-295. https://doi.org/10.1016/j.icheatmasstransfer.2019.104295

[5] Madhu M., Shashikumar N.S., Gireesha B.J. and Kisha B.J. (2019): *Second law analysis of Powell-Eyring fluid flow through an inclined microchannel with thermal radiation.–* Physica Scripta, vol.94, pp.125-205, https://ui.adsabs.harvard.edu/link_gateway/2019PhyS...94l5205M/doi:10.1088/1402-4896/ab32b7

[6] Madhu M., Shashikumar N.S., Mahanthesh B., Gireesha B.J. and Kishan N. (2019): *Heat transfer and entropy generation analysis of non-Newtonian fluid flow through vertical microchannel with convective boundary condition.–* Applied Mathematics and Mechanics, vol.40, pp.1285-1300, https://doi.org/10.1007/s10483-019-2516- 9

[7] Akbar Y., Abbasi F.M. and Shehzad S.A. (2020): *Thermal radiation and Hall efects in mixed convective peristaltic transport of nanofuid with entropy generation.–* Applied Nanoscience, vol.10, pp.5421-5433, https://doi.org/10.1007/s13204-020-01446-3

[8] Matin M.H., Nobari M.R.H and Jahangiri P. (2012): *Entropy analysis in mixed convection MHD flow of nanofluid over a non-linear stretching sheet.*– Journal of Thermal Science and Technology, vol.7, pp.104-119, https://doi.org/10.1299/jtst.7.104

[9] BiancoV., Manca O. and Nardini S. (2014): *Entropy generation analysis of turbulent convection flow of Al_2O_3–water nanofluid in a circular tube subjected to constant wall heat flux.*– Energy Conversion and Management, vol.77, pp.306-314, https://doi.org/10.1016/j.enconman.2013.09.049

[10] Das S., Chakraborty S. and Jana R.N. (2021): *Entropy analysis of Poiseuille nanofluid flow in a porous channel with slip and convective boundary conditions under magnetic field.*– World Journal of Engineering, https://doi.org/10.1108/WJE-12-2020-0660

[11] Shah Z., Kumam P. and Deebani W. (2020): *Radiative MHD Casson nanofuid flow with activation energy and chemical reaction over past nonlinearly stretching surface through entropy generation.*– Scientific Report, vol.10, pp.1-14, https://doi.org/10.1038/s41598-020-61125-9

[12] Mirzaee M. and Lakzian E. (2017): *Entropy generation analysis of eccentric cylinders pair sources on nanofluid natural convection with non-Boussinesq state.*– Tech. Adv. Powder, vol.28, pp.3172-3183. https://doi.org/10.1016/j.apt.2017.09.034

[13] Hosseinzadeh K., Asadi A., Mogharrebi A.R., Khalesi J., Mousavisani S. and Ganji. D.D. (2019): *Entropy generation analysis of $(CH_2OH)_2$ containing CNTs nanofluid flow under effect of MHD and thermal radiation.*– Case Studies in Thermal Engineering, vol.14, pp.100-482, https://doi.org/10.1016/j.csite.2019.100482

[14] Ibáñez G., López A., Pantoja J. and Moreira J. (2016): *Entropy generation analysis of a nanofluid flow in MHD porous microchannel with hydrodynamic slip and thermal radiation.*– Int. J. Heat Mass Trans., vol.100, pp.89-97, https://doi.org/10.1016/j.ijheatmasstransfer.2016.04.089

[15] Daniel Y.S., Aziz Z.A., Ismail Z. and Salah F. (2017): *Entropy analysis in electrical magnetohydrodynamic (MHD) flow of nanofluid with effects of thermal radiation, viscous dissipation, and chemical reaction.*– Theoretical & Applied Mechanics Letters, vol.7, pp.235-242, https://doi.org/10.1016/j.taml.2017.06.003

[16] Hussain S., Mehmood K., and Sagheer M. (2016): *MHD mixed convection and entropy generation of water–alumina nanofluid flow in a double lid driven cavity with discrete heating.*– Journal of Magnetism and Magnetic Materials, vol.419, pp.140-155, https://doi.org/10.1016/j.jmmm.2016.06.006

[17] Tayebi T. and Chamkha A.J. (2019): *Entropy generation analysis during MHD natural convection flow of hybrid nanofluid in a square cavity containing a corrugated conducting block.*– International Journal of Numerical Methods for Heat & Fluid Flow, vol.30, pp.1115-1136, https://doi.org/10.1108/HFF-04-2019-0350

[18] Roja A., Gireesha B.J. and Prasannakumara B.C. (2020): *MHD micropolar nanofluid flow through an inclined channel with entropy generation subjected to radiative heat flux, viscous dissipation and multiple slip effects.*– Multidiscipline Modeling in Materials and Structures, vol.16, pp.1475-1496, https://doi.org/10.1108/MMMS-12-2019-0235

[19] Javed T. and Siddiqui M.A. (2019): *Mixed convection in micropolar nanofluid flow through entraed triangular enclosures and linear stability analysis considering magnetic effects and heat generation and absorption.*– Canadian Journal of Physics, vol.97, pp.252-266, https://doi.org/10.1139/cjp-2017-0974

[20] Javed T., Mehmood Z. and Siddiqui M.A. (2017): *Mixed convection in a triangular cavity permeated with micropolar nanofluid-saturated porous medium under the impact of MHD.*– Journal of the Brazilian Society of Mechanical Sciences and Engineering, vol.39, pp.3897-3909, https://doi.org/10.1007/s40430-017-0850-5

[21] Chand R., Yadav D., Bhattacharyya K. and Awasthi M.K. (2021): *Thermal convection in a layer of micropolar nanofluid.*– Chemical engineering, vol.16, p.2681. https://doi.org/10.1002/apj.2681

[22] Yusuf T.A., Kumar R.N., Prasannakumara B.C. and Adesanya S.O. (2021): *Irreversibility analysis in micropolar fluid film along an incline porous substrate with slip effects.*– International Communications in Heat and Mass Transfer, vol.126, pp.105-357, https://doi.org/10.1016/j.icheatmasstransfer.2021.105357

[23] Ramesh G.K., Rauf A., Shehzad S.A. and Abbasi F.M. (2021): *Time-dependent squeezing flow of Casson-micropolar nanofluid with injection/suction and slip effects.*– International Communications in Heat and Mass Transfer, vol.126 pp.104-470. https://doi.org/10.1016/j.icheatmasstransfer.2021.105470

[24] Ijazkhan M., Waqas H., Khan S.U., Imran M., Chu Y.M., Abbasi A. and Kadry S. (2021): *Slip flow of micropolar nanofluid over a porous rotating disk with motile microorganisms, nonlinear thermal radiation and activation energy.*– International Communications in Heat and Mass Transfer, vol.122, pp.105-161. https://doi.org/10.1016/j.icheatmasstransfer.2021.105161

[25] Eid M.R and Mabood F. (2021): *Entropy analysis of a hydromagnetic micropolar dusty carbon NTs-kerosene nanofluid with heat generation: Darcy–Forchheimer scheme.–* Journal of Thermal Analysis and Calorimetry, vol.143, pp.2419-2436, https://doi.org/10.1007/s10973-020-09928-w

[26] Almakki M., Mondal H. and Sibanda P. (2021): *Onset of unsteady MHD micropolar nanofluid flow with entropy generation.–* International Journal of Ambient Energy, pp.1-14, https://doi.org/10.1080/01430750.2021.1890213

[27] Zaib A., Khan U., Shah Z., Kumam P. and Thounthong P. (2019): *Optimization of entropy generation in flow of micropolar mixed convective magnetite (Fe₃O₄) ferroparticle over a vertical plate.–* Alexandria Engineering Journal, vol.58, No.4, pp.1461-1470, https://doi.org/10.1016/j.aej.2019.11.019

[28] Nayak M.K., Mabood F., Khan W.A. and Makinde O.D. (2021) : *Cattaneo–Christov double diffusion on micropolar magneto cross nanofluids with entropy generation.–* Indian Journal of Physics, pp.1-16, https://doi.org/10.1007/s12648-020-01973-3

[29] Hsiao L. (2010): *Heat and mass transfer for micropolar flow with radiation effect past a nonlinearly stretching sheet.–* Heat Mass Transfer, vol. 46, pp.413-419, https://doi.org/10.1007/s00231-010-0580-z

[30] Yacob N.A. and Ishak A. (2011): *MHD flow of a micropolar fluid towards a vertical permeable plate with prescribed surface heat flux.–* Chemical Engineering Science Research Design, vol.89, pp.2291-2297, https://doi.org/10.1016/j.cherd.2011.03.011

[31] Woods L.C. (2006) *Thermodynamics of Fluid Systems.–* Oxford University Press, Oxford

[32] Alam M.S., Rahman M.M. and Sattar M.A. (2009): *On the effectiveness of viscous dissipation and Joule heating on steady magnetohydrodynamic heat and mass transfer flow over an inclined radiate isothermal permeable surface in the presence of thermophoresis.–* Communications in Nonlinear Science and Numerical Simulation, vol.14, pp.2132-2143, https://doi.org/10.1016/j.cnsns.2008.06.008